Available online at www.sciencedirect.com
SCIENCE DIRECT®
Journal of Catalysis 231 (2005) 259–268
JOURNAL OF CATALYSIS
www.elsevier.com/locate/jcat

The effect of phosphate and glycol on the sulfidation mechanism of $CoMo/Al_2O_3$ hydrotreating catalysts: an in situ QEXAFS study

Daniele Nicosia, Roel Prins *

Institute for Chemical and Bioengineering, Federal Institute of Technology (ETH), 8093 Zurich, Switzerland

Received 22 November 2004; revised 12 January 2005; accepted 17 January 2005

Available online 17 March 2005

Abstract

The sulfidation of $CoMo/\gamma\text{-}Al_2O_3$ catalysts prepared in the presence of phosphate and triethylene glycol (TEG) was studied by in situ Mo and Co K-edge QEXAFS. In a classic CoMo catalyst, prepared without phosphate and TEG, MoS_2 is formed through intermediate MoS_3-like species. In the presence of phosphate, alone or with TEG, this intermediate species is not observed and the molybdenum is directly sulfided to MoS_2. The additives increased the sulfidation degree of molybdenum with respect to the standard catalyst, leading to a better sulfur saturation of the MoS_2 slabs and to a higher static order. Co K-edged QEXAFS showed that the sulfidation rate of Co increases in the presence of phosphate and TEG.

Keywords: Triethylene glycol; Phosphomolybdate species; CoMo HDS catalysts; In situ QEXAFS

1. Introduction

Hydrodesulfurization (HDS) is the most important catalytic process for the removal of sulfur from petroleum. When organic sulfur-containing molecules are burned in industrial plants or in the engines of automobiles, sulfur oxides are released into the atmosphere. These sulfidic compounds may further react with water in the atmosphere to form sulfuric acid and, as a consequence, increase acid rain. As legislation concerning the emission of sulfur-containing pollutants is becoming stricter, the HDS process must be improved. One way to achieve this goal is to improve the reactivity of CoMo and NiMo HDS catalysts by looking for new preparation routes or by adding doping agents.

A fundamental step in the preparation of HDS catalysts is pre-sulfidation, which is carried out right before the catalysts are used in the hydrotreating reactions and in which the oxidic precursors are converted into the final sulfidic catalyst. Several studies have been published on the mechanism of sulfidation of the HDS catalysts. In these studies various techniques, such as temperature-programmed sulfidation [1], laser Raman spectroscopy [2], and extended X-ray absorption fine structure (EXAFS) [3,4], have been used. As pre-sulfidation is a dynamic process, it is mandatory to use an in situ technique to obtain reliable results. Cattaneo et al. and Sun et al. recently performed several in situ experiments with the Quick-EXAFS technique to characterize various steps of sulfidation of Co (Ni) and Mo (W) catalysts containing doping agents such as fluorine and chelating ligands [5,6].

To obtain a better understanding of the processes involved in the production of more active hydrotreating catalysts, we previously investigated the structure of oxidic CoMo catalysts containing phosphate and triethylene glycol (TEG) [7], prepared according to a recently released patent [8]. The work presented here furthers the understanding of this system by reporting the use of in situ Mo and Co K-edge QEXAFS to determine how the mechanism of sulfidation is influenced by the presence of phosphate and triethylene glycol.

* Corresponding author. Fax: +41-1-6321162.
E-mail address: roel.prins@chem.ethz.ch (R. Prins).

0021-9517/$ – see front matter
doi:10.1016/j.jcat.2005.01.018

2. Experimental

2.1. Sample preparation and characterization

The wet impregnation method was used to prepare CoMoP/γ-Al_2O_3 and CoMoP-TEG/γ-Al_2O_3 (containing triethylene glycol, TEG), according to the European patent application 0601722 B1 [8] and our previous publication [7]. In short, 2.7 g MoO_3 powder (18.7 mmol, Fluka, purum, p.a.) and 0.5 ml of an 85 wt% aqueous H_3PO_4 solution (7.5 mmol H_3PO_4, Aldrich, p.a.) were dissolved in 10 ml water with stirring and refluxing at 80 °C for one night. The solution was cooled to room temperature, 1 g $CoCO_3$ (8.5 mmol, Aldrich p.a.) was added, and the solution was stirred for 3 h; upon the addition of the cobalt salt, CO_2 evolved. The resulting solution was red and the pH was 3.0. In the case of the CoMoP-TEG impregnation solution, 2 ml TEG (15 mmol, Aldrich, p.a.) was added after the $CoCO_3$ was dissolved. No changes in pH or color were observed after the addition of the glycol. These catalysts were compared with classical CoMo/γ-Al_2O_3 and CoMo-TEG/γ-Al_2O_3 catalysts, which we prepared by dissolving 2.7 g MoO_3, 2.5 g $Co(NO_3)_2 \cdot 6H_2O$, and 2 ml TEG in 10 ml 25% aqueous NH_3 solution (Fluka, purum, p.a.); the pH of the solution was 9. Before impregnation with one of the solutions, the γ-Al_2O_3 (Condea Chemie) was crushed, sieved (90–125-μm grain size), and dried overnight in an oven at 120 °C. The total water pore volume of the dried γ-Al_2O_3 was 0.9 ml/g. The impregnation of the support was carried out by the dropwise addition of 0.9 ml of the impregnation solution over the dried γ-Al_2O_3. After stirring for 1 h, the wet powder was transferred to an oven and dried at 120 °C (ramp 2 °C/min) for 16 h. Calcination was not applied.

The investigated catalyst precursors are listed in Table 1. Atomic absorption spectroscopy was performed with a Varian SpectraAA 200FS atomic absorption spectrometer, equipped with a hollow tube lamp, which emitted the Co and Mo wavelengths at 240.7 and 313.3 nm, respectively. To measure the phosphorus content, a photometric method was employed [7]. Nitrogen adsorption measurements of the dry but not calcined samples were performed at liquid-nitrogen temperature with a Micromeritics TriStar 3000. Because no calcination was performed, the BET surface area of the CoMo/γ-Al_2O_3 catalysts was only 115 m^2/g, whereas the calcined CoMo/γ-Al_2O_3 catalyst had a BET surface area of 177 m^2/g. The surface areas were determined from the nitrogen adsorption isotherms, according to the BET method, and the pore size distribution was determined from the desorption branches of the isotherms according to the BJH method.

The catalytic tests of our samples were performed with an apparatus that was a modified version of a flow system described elsewere [9]. An amount of 0.1 g of each oxidic precursor was diluted in 0.9 g of SiC and sulfided at 400 °C (heating rate 6 °C/min) for 2 h with a mixture of 10% H_2S in H_2 (Messer Griesheim 3.0). The sulfiding mixture flowed through the reactor at 60 ml/min from the beginning of the heating process. The activity of all of the catalysts was tested in the HDS of thiophene at 350 °C [5]. We obtained the feed, consisting of 3% thiophene in H_2, by bubbling H_2 through a series of four thiophene saturators, which were cooled to 2 °C. The thiophene/H_2 mixture flowed over the catalyst at 75 ml/min, corresponding to a GHSV of 22,000 h^{-1}. Further details regarding the activity test can be found in [7].

The conversion of all of the catalysts was normalized for the Co + Mo loading of the oxidic catalyst precursor to directly compare catalysts with a slightly different metal loading.

2.2. XAFS measurements and data analysis

We carried out in situ Mo and Co K-edge classical EXAFS and QEXAFS at the X1 beam line at HASYLAB (Hamburg, Germany) to follow the sulfidation of CoMo catalysts supported on γ-Al_2O_3 in the presence and absence of phosphate and triethylene glycol. The energy of the beamline ranges from 6 to 70 keV [10] and is regulated by a continuously moving two-crystal monochromator [11]. The monochromator is equipped with three parallel mounted pairs of Si(111), Si(311), and Si(511) crystals. The first crystal was detuned with respect to the second one to eliminate higher orders of diffraction in the transmitted beam, so that the intensity of the exit X-ray beam was 70% of the original. The Si(311) and the Si(111) crystals were used for the Mo and Co K-edges, respectively, and the accumulation time was about 0.3 s/step at both edges.

The catalyst samples were pressed into self-supporting wafers and mounted in the in situ EXAFS cell [12]. The thickness of the sample was chosen to adjust the edge jump to 1. We carried out the sulfidation by flushing the cell with a 10% H_2S/H_2 mixture while heating to 400 °C at 6 °C/min. Classical EXAFS measurements of the sulfided samples were carried out at liquid nitrogen temperature in

Table 1
CoMo hydrotreating catalysts doped with phosphate and triethylene glycol

Catalyst	Loading (wt%)			Co/Mo mol ratio	P/Mo mol ratio	BET s.a. (m^2/g)	P.V. (m^3/g)	Av. P.D. (nm)	Conversion/ Co + Mo (g^{-1})
	Mo	Co	P						
CoMo/γ-Al_2O_3	12.30	2.60	–	0.34	–	115	0.25	5.8	1.6
CoMo-TEG/γ-Al_2O_3	12.40	2.49	–	0.31	–	90	0.21	5.3	1.7
CoMoP/γ-Al_2O_3	12.85	2.88	1.75	0.37	0.42	144	0.32	6.3	2.4
CoMoP-TEG/γ-Al_2O_3	12.47	2.86	1.60	0.37	0.40	114	0.28	5.7	2.8

static He after the H_2/H_2S mixture was evacuated from the cell.

EXAFS data analyses were carried out with the XDAP (version 2.2.3) program [13], according to the procedure described in [14]. For the analysis of the Mo–O, Mo–Mo, Mo–S, and Mo–P contributions, EXAFS data from the following experimental reference compounds were used: Na_2MoO_4 for the Mo–O contributions, MoS_2 for the Mo–Mo and Mo–S contributions, and MoP for the Mo–P contribution. For other Mo–X contributions, the FEFF 8 code was used to generate theoretical references [15]. MoP was prepared by direct reduction of amorphous molybdenum phosphate [16]. The calibration of the references was carried out as described in [17]. Similar to the XAFS spectra of the catalysts, the reference spectra were measured at liquid nitrogen temperature, thus optimizing the references for the data analysis.

3. Results

3.1. HDS activity

Table 1 shows the HDS activities of the catalysts under study. As shown previously, there is a synergistic effect of phosphate and triethylene glycol, which leads to the highest activity for CoMoP-TEG/γ-Al_2O_3 [7]. It was proposed that triethylene glycol interacts strongly with γ-Al_2O_3, preventing the decomposition of the Co-diphosphopentamolybdate complex on the surface of the support. This leads to the stabilization of a Co-diphosphopentamolybdate species on the support, in which cobalt and molybdenum are in close proximity, thus facilitating the formation of the most active Co–Mo–S structure and leading to an increase in the catalytic activity.

3.2. Mo K-edge Quick EXAFS

Figs. 1A and 1B show the sulfidation process of Mo in the CoMo/γ-Al_2O_3 catalyst as monitored by a series of Fourier transforms of the Quick EXAFS scans. Whereas the first Fourier transform is that of the untreated sample at room temperature, the others were collected at increasing temperature upon sulfidation with the H_2S/H_2 mixture. The numbers on the ordinates indicate the average temperature ranges during the scan. In the Fourier transform of the spectrum of the fresh catalyst, the signal between 0.6 and 2.5 Å can be assigned to the octahedral coordination of the Mo absorber atom by oxygen atoms. The signal between 3.1 and 3.7 Å arises from a Mo–Mo shell, which suggests the presence of polymolybdate in the catalyst precursor. The same result was reported by Cattaneo et al. for a NiMo catalyst supported on γ-Al_2O_3 [18]. Fig. 1A shows that, despite the sulfiding treatment, the oxidic phase is stable up to about 108 °C. However, both Mo–O and Mo–Mo signals broaden, and, at the same time, a new signal appears between 1.8 and 2.5 Å. The effect of sulfidation becomes evident in the Fourier transform of the spectrum measured at 132 °C (Fig. 1B). At this stage, the new signal between 1.8 and 2.5 Å has clearly replaced the original Mo–O signal, and the signal corresponding to the Mo–Mo shell of the polymolybdate has disappeared. The signal between 1.0 and 1.8 Å, due to Mo–O contributions, is still present, however. The new signal between 1.8 and 2.5 Å was also observed by Cattaneo et al., who attributed it to the

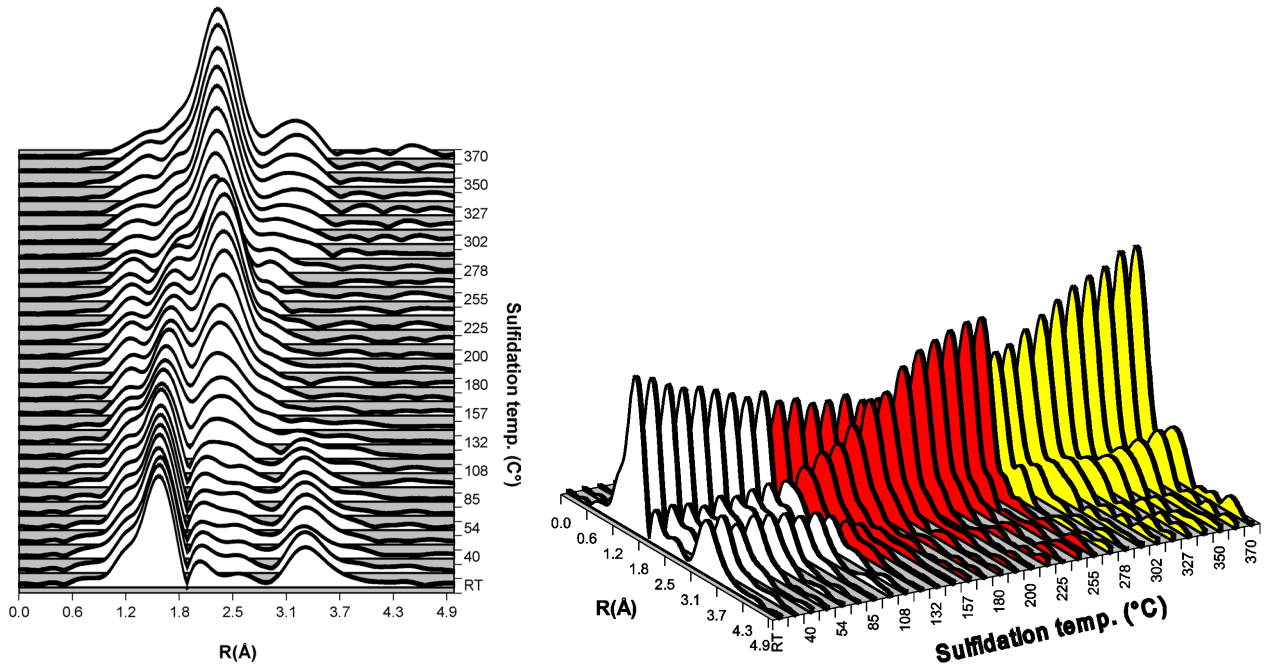

Fig. 1. Fourier transforms of in situ Mo K-edge QEXAFS during the heating of CoMo/γ-Al_2O_3 in a flow of H_2S and H_2.

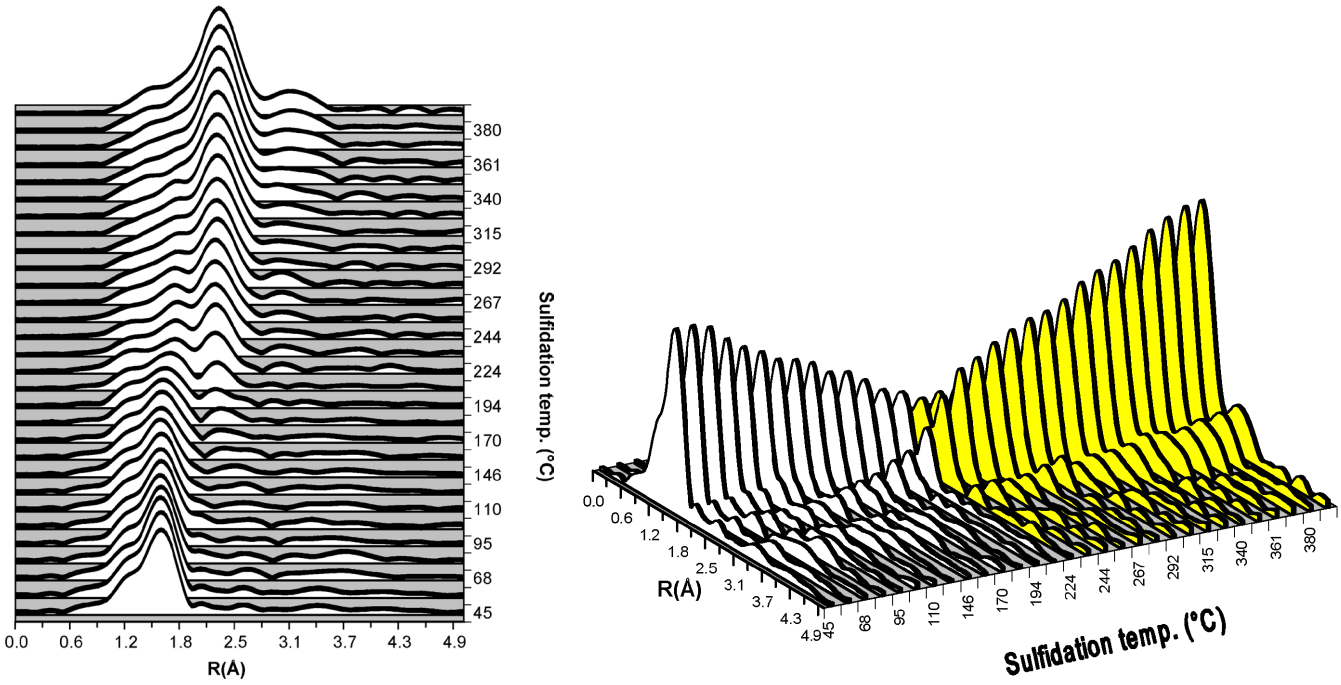

Fig. 2. Fourier transforms of the in situ Mo K-edge QEXAFS during the heating of CoMoP/γ-Al_2O_3 in a flow of H_2S and H_2.

Mo–S shell of an MoS_3-like species [18]. The signal of this species reaches a maximum at 255 °C (Fig. 1B). Moreover, a shoulder at about 3 Å, which arises from the Mo–Mo contribution of MoS_3, is visible as well.

When the temperature increases further, the coordination of Mo changes again. The amplitude of the Mo–S signal suddenly moves from about 2.5 Å to a lower value (Fig. 1A) and decreases substantially (Fig. 1B). At the same time, the Mo–Mo signal moves from about 3 Å to a higher value. This indicates that the MoS_3-like species has decomposed to the more stable MoS_2. The amplitudes of the Mo–S and Mo–Mo signals of MoS_2 increase with increasing sulfidation temperature, demonstrating the growth of the MoS_2 crystallites. Also in the presence of TEG in the CoMo-TEG/γ-Al_2O_3 sample, the same three phases were observed in the QEXAFS sulfidation patterns (not shown here).

The effect of phosphate on the sulfidation of the CoMoP/γ-Al_2O_3 catalyst is shown in Figs. 2A and 2B. A Raman and Mo K-edge EXAFS spectroscopy study of the structure of this catalyst precursor showed that the diphosphopentamolybdate anions in the impregnation solution decomposed to phosphoaluminate and aluminum molybdate when the solution came into contact with γ-Al_2O_3 [7]. The FT of the Mo EXAFS of the oxidic CoMoP/γ-Al_2O_3 sample (Fig. 2A) mainly shows a large signal between 0.6 and 1.8 Å, corresponding to Mo atoms tetrahedrally coordinated by oxygen atoms, and a weak signal between 3.1 and 3.7 Å is due to a Mo–Al contribution [7]. In this chemical environment, molybdenum is affected by the sulfiding treatment at about 190 °C. In the Fourier transform of the spectrum collected at this temperature, the signal due to the oxygen shell is very broad, and a Mo–S contribution is present between 1.8 and 2.5 Å. Moreover, a signal at about 3 Å, arising from a Mo–Mo contribution, appears at about 250 °C. These contributions increased steadily in intensity until the end of the sulfiding treatment, and no intermediates formed. At the end of the sulfidation MoS_2 was detected.

Figs. 3A and 3B show the sulfidation of the CoMoP-TEG/γ-Al_2O_3 catalyst. As previously reported [7], the molybdenum in the oxidic precursor is mainly present as a cobalt phosphomolybdate salt. The signal between 0.9 and 1.8 Å is due to the octahedrally coordinated oxygen shell, whereas the signals at 3.1 and 4.2 Å result from the overlap between the Mo–Mo and Mo–P contributions. Fig. 3A shows that these signals broaden with increasing sulfidation temperature. At 215 °C a signal corresponding to a Mo–S contribution appears at about 2.1 Å. Although at this temperature the Mo–Mo and Mo–P signals disappear, a very broad Mo–O contribution is still present. At 240 °C an additional peak, arising from a Mo–Mo contribution, is present at about 2.9 Å. When the sulfidation temperature increases above 324 °C, the Mo–O signal disappears and the Mo–Mo contribution moves to a larger distance.

Fig. 4 shows the increase in the Mo–S coordination number, as obtained by quantitative analysis of each QEXAFS spectrum versus the sulfidation temperature for all four catalysts. The trend of the Mo–S coordination number of the CoMo/γ-Al_2O_3 and CoMo-TEG/γ-Al_2O_3 samples with increasing sulfidation temperature is very similar to that shown by Cattaneo et al. for the sulfidation of NiMo catalysts supported on γ-Al_2O_3 containing various amounts of chelating ligands like NTA and EDTA [18]. The Mo–S coordination

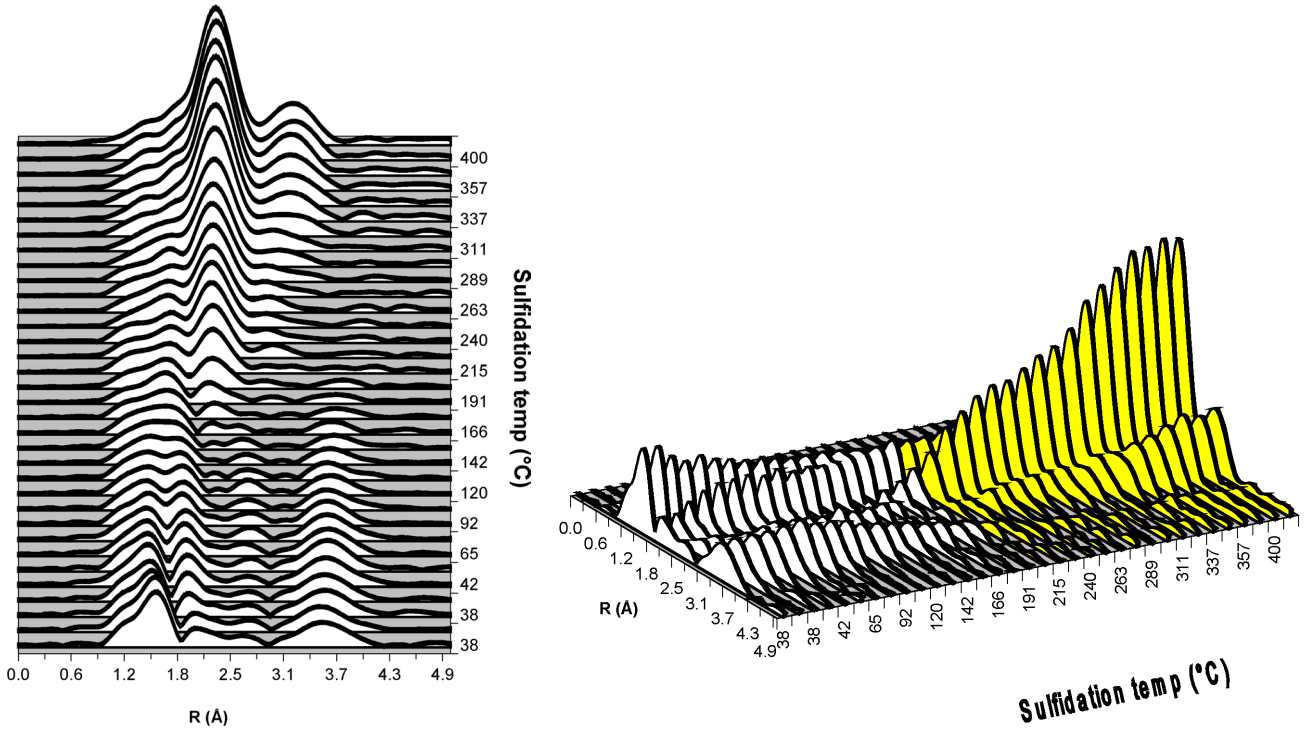

Fig. 3. Fourier transforms of the in situ Mo K-edge QEXAFS during the heating of CoMoP-TEG/γ-Al_2O_3 in a flow of H_2S and H_2.

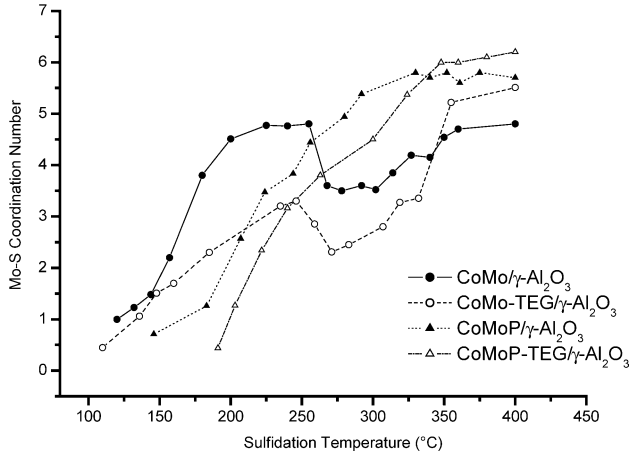

Fig. 4. Mo–S coordination numbers resulting from the Mo K-edge QEXAFS data fits.

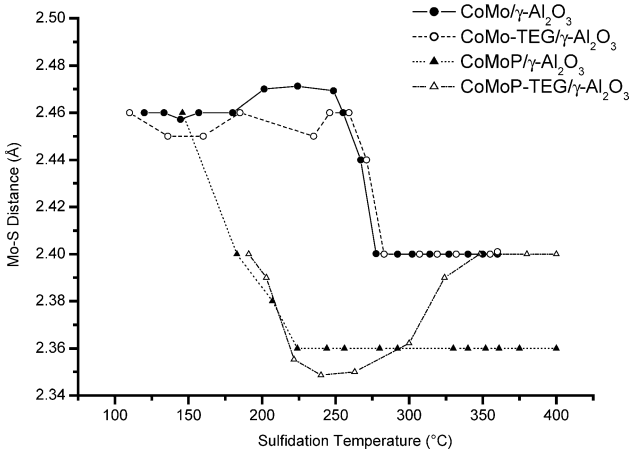

Fig. 5. Mo–S distance resulting from the Mo K-edge QEXAFS data fits.

number reaches a maximum at about 250 °C. At this temperature the Mo–S coordination number in the CoMo/γ-Al_2O_3 sample is 4.7. At higher temperatures it drops to 3.5, and at about 350 °C it increases again to 4.8. In the case of the CoMo-TEG/γ-Al_2O_3 sample, the Mo–S coordination is 3.3 at about 250 °C; at higher temperatures it first decreases to 2 and then increases to 5.5. In the case of the CoMoP/γ-Al_2O_3 and CoMoP-TEG/γ-Al_2O_3 samples, the trend is more continuous than in the phosphate-free samples. The Mo–S coordination numbers of both catalysts increase continuously and reach a plateau of about 6. The plots of the Mo–S distance as a function of the sulfiding temperature (Fig. 5) show that in the phosphate-free CoMo/γ-Al_2O_3 and CoMo-TEG/γ-Al_2O_3 samples, a Mo–S contribution was already observed at 100 °C. The corresponding signals, probably due to a MoS_3-like species, increase in intensity up to 250 °C but suddenly broaden at higher temperatures, shift to shorter distance values, and finally remain stable until the end of the treatment (Figs. 1A and 1B). At this stage the presence of MoS_2 is detected. In summary, the formation of MoS_2 in the phosphate-free samples took place through the formation of an MoS_3-like intermediate, which decomposed at about 250 °C.

The sulfidation is different in the case of the phosphate-containing CoMoP/γ-Al_2O_3 and CoMoP-TEG/γ-Al_2O_3

Table 2
Structural parameters resulting from the Mo K-edge Fourier-filtered k^3-weighted EXAFS functions of the final sulfided catalysts ($\Delta R = 0.5$–3.3 Å)

Catalyst	Shell	Coordination number N (±10%)	Coordination distance R (Å) (±1%)	Debye–Waller factor $10^3\Delta\sigma^2$ (Å^2) (±5%)	Energy shift ΔE_0 (eV) (±10%)	Goodness of fit (ε_ν^2)
CoMo/γ-Al_2O_3	Mo–S	4.8	2.41	4.3	−7.0	0.79
	Mo–Mo	2.5	3.18	8.1	−7.8	
CoMo-TEG/γ-Al_2O_3	Mo–S	5.5	2.40	4.8	−5.2	0.9
	Mo–Mo	3.6	3.17	9.6	5.5	
CoMoP/γ-Al_2O_3	Mo–S	5.8	2.36	8.3	−2.1	0.14
	Mo–Mo	1.9	3.15	8.4	−1.0	
CoMoP-TEG/γ-Al_2O_3	Mo–S	6.0	2.40	5.7	−2.6	0.23
	Mo–Mo	3.0	3.17	6.8	−5.0	

catalysts. The CoMoP/γ-Al_2O_3 catalyst starts to show a Mo–S contribution at 150 °C, probably arising from the MoS_2 species [19]. Between 150 and 225 °C the Mo–S distance decreases steeply from 2.46 to 2.36 Å; this value remains constant until the end of the treatment. The presence of TEG in the CoMoP-TEG/γ-Al_2O_3 sample had a different effect on the sulfidation of this catalyst precursor (Fig. 5). A Mo–S contribution at 2.40 Å was detectable at about 175 °C, which shortened to 2.35 Å at 255 °C and increased to 2.40 Å with a further increase in temperature. The distance of 2.40 Å was the same as that found at the end of the sulfidation of the CoMo/γ-Al_2O_3 and CoMo-TEG/γ-Al_2O_3 samples.

3.3. Mo K-edge EXAFS

We performed classical EXAFS measurements of the four catalysts at 400 °C, while flushing with the H_2/H_2S mixture. The results of the data analyses show that the sulfided noncalcined CoMo/γ-Al_2O_3 catalyst has the lowest Mo–S coordination number (Table 2). This indicates that either not all of the MoS_2 crystallite edges are saturated with S or that some of the Mo edge atoms are coordinated to oxygen. In the presence of phosphate and/or TEG, the Mo–S coordination number increases, reaching full octahedral coordination for CoMoP-TEG/γ-Al_2O_3. Three of the four catalysts have a Mo–S distance of 2.41 Å, typical of the 2H–MoS_2 phase. Only the CoMoP/γ-Al_2O_3 sample showed a Mo–S distance of 2.36 Å, which is typical of the Mo–S distance in the 3R–MoS_2 phase [20], as calculated from the crystallographic data available in the ICSD database [21]. Comparison of the Mo–Mo coordination numbers and the Debye–Waller factors enables us to evaluate the state of static order and crystallinity of the MoS_2 slabs. The CoMo/γ-Al_2O_3 sample has a Mo–Mo coordination number of 2.5, corresponding to a MoS_2 crystallite size of 20 Å [22]. The rather high Debye–Waller factor, calculated from the data fit, indicates that MoS_2 in this catalyst has a low static order. As shown in Table 2, phosphate and TEG have an opposite effect on the Mo–Mo coordination number. Whereas the Mo–Mo coordination number of the CoMo-TEG/γ-Al_2O_3 sample is 3.6, it is 1.9 in the CoMoP/γ-Al_2O_3. However, the high

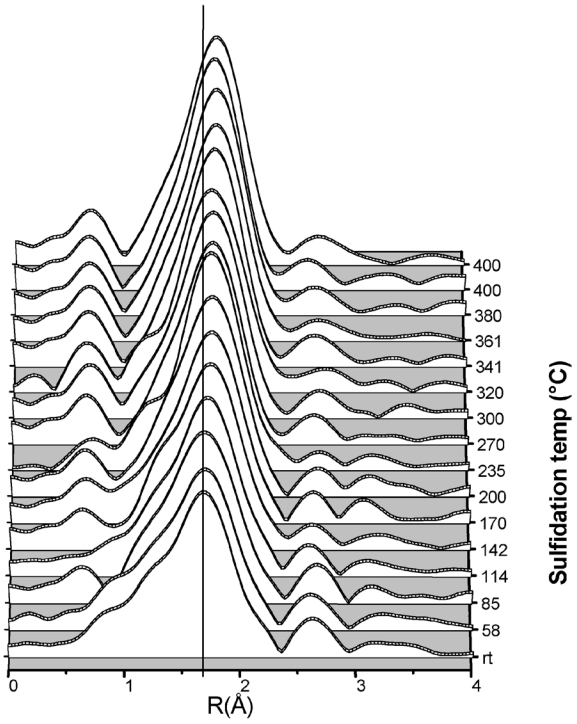

Fig. 6. Fourier transforms of the in situ Co K-edge QEXAFS during the heating of CoMo/γ-Al_2O_3 in a flow of H_2S and H_2.

Debye–Waller factor revealed that, in the presence of TEG, the MoS_2 crystallites have an even lower static order than in the CoMo/γ-Al_2O_3 catalyst. The presence of phosphate and TEG in the catalyst has, however, a beneficial effect on the CoMoP-TEG/γ-Al_2O_3 catalyst, since this catalyst has the lower Debye–Waller factor, indicating a better static order (Table 2).

3.4. Co K-edge Quick EXAFS

The sulfidation of Co in the catalysts was investigated by means of Co K-edge QEXAFS (Fig. 6). The Fourier transform of the QEXAFS of the fresh CoMo/γ-Al_2O_3 catalyst shows a large signal between 0.5 Å and about 2.5 Å, which is due to a Co–O contribution. A small peak is also present between 2.3 and 3 Å, probably due

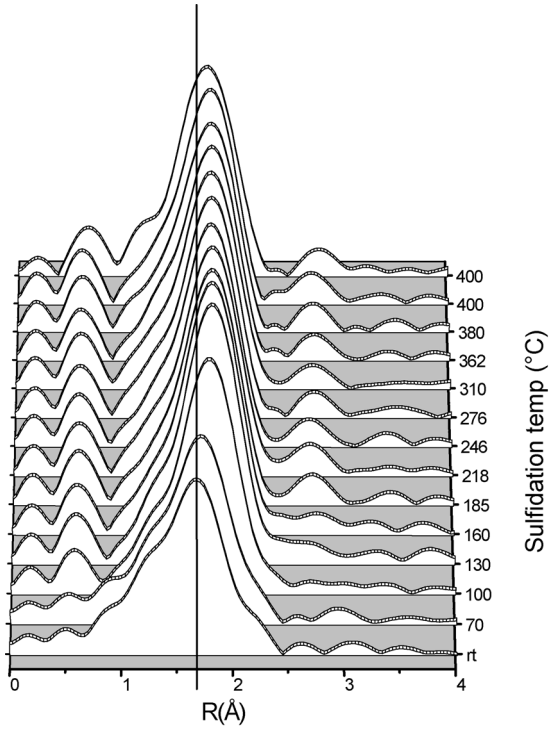

Fig. 7. Fourier transforms of the in situ Co K-edge QEXAFS during the heating of CoMoP/γ-Al_2O_3 in a flow of H_2S and H_2.

to a Co–Al contribution. At about 142 °C the Co–O peak starts to shift to a larger distance; this indicates that oxygen is being replaced by sulfur. Fig. 7 shows the FT of the Co K-edge QEXAFS of CoMoP/γ-Al_2O_3. The fresh catalyst shows one signal corresponding to a Co–O contribution but no signal at larger distances. For this catalyst oxygen is being replaced by sulfur already at 100 °C. The sulfidation of CoMo-TEG/γ-Al_2O_3 and CoMoP-TEG/γ-Al_2O_3 (both not shown here) showed hardly any differences from the trend observed for the previous catalysts.

A more precise picture of the sulfidation of Co in the four catalysts is achieved by monitoring of the XANES spectra. The XANES spectra of the fresh oxidic CoMoP/γ-Al_2O_3 sample are characterized by a white-line feature around 7725 eV, which decreases in intensity with increasing temperature (Fig. 8). At the end of the sulfidation, the white line totally disappeared. By means of a linear combination fit, it is possible to evaluate the sulfidation rate of Co in the catalyst [23]. The spectrum of a sulfided sample is considered to consist of a linear combination of the spectrum of the fresh oxidic catalyst and the spectrum collected after sulfid ation at 400 °C. The results for all four catalysts are shown in Fig. 9. It is clear that the presence of phosphate and TEG increases the sulfidation Co in the catalysts.

4. Discussion

In this section we discuss the effect of phosphate and glycol on the mechanism of sulfidation of molybdenum and cobalt. The results are correlated with the HDS activity.

4.1. Molybdenum

The results obtained for the sulfidation of noncalcined CoMo/γ-Al_2O_3 are consistent with those obtained by Cattaneo et al. for noncalcined NiMo/γ-Al_2O_3 [18]. We recognized three temperature regions during the sulfidation of

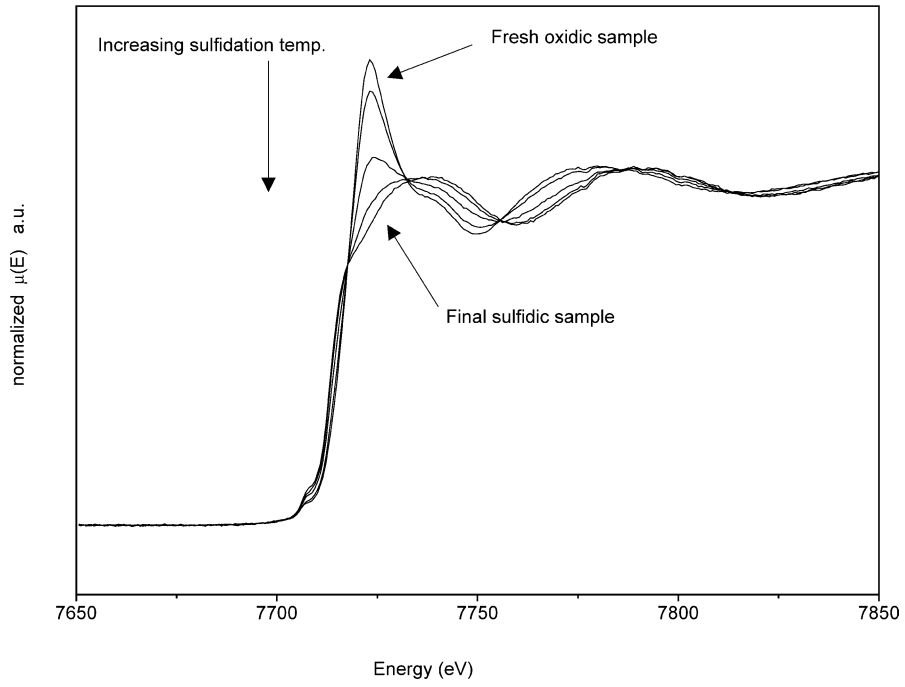

Fig. 8. Normalized in situ Co K-edge XANES during the heating of CoMoP/γ-Al_2O_3 in a flow of H_2S and H_2.

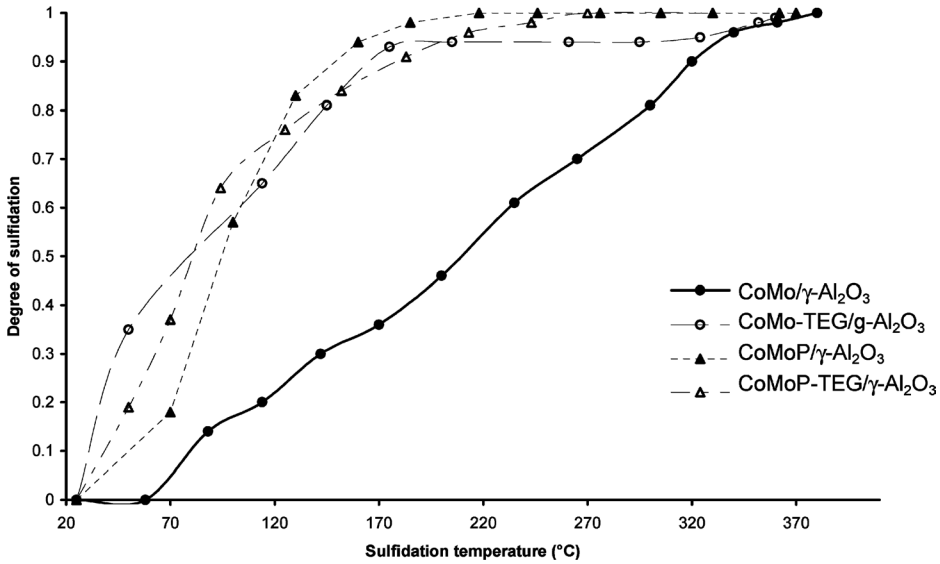

Fig. 9. Degree of sulfidation of Co in the CoMo catalysts as obtained by a linear combination fit of the Co K-edge XANES spectra of fresh oxidic and final sulfided sample.

CoMo/γ-Al_2O_3. The first region is related to oxidic molybdenum arising from polymolybdate, the formation of which was favored by the basic pH of the impregnation solution. Because of the high pH, the γ-Al_2O_3 surface was negatively charged, preventing a good dispersion of the molybdate and inducing it to polymerize on the surface of the support. The second region in the QEXAFS was attributed by Cattaneo et al. to a MoS_3-like species. As shown in Figs. 1A and 1B, this phase is stable up to 255 °C; at higher temperature it decomposes to MoS_2. However, the low Mo–S coordination number, obtained from the EXAFS data analysis (Table 2), indicates that the MoS_2 slabs are not fully saturated by sulfur. This might be due to the presence of Mo–O–Al bonds of Mo atoms at the edges of MoS_2 on the alumina support, which are very difficult to cleave. In the sulfidation of the CoMo-TEG/γ-Al_2O_3 sample, we observed the same sequence of three phases: polymolybdate, a MoS_3-like phase, and MoS_2. At low-temperature TEG decreases the degree of Mo sulfidation of the initial MoS_3-like phase in CoMo-TEG/γ-Al_2O_3 (Fig. 4). However, at the end of the sulfiding treatment, the Mo–S and Mo–Mo coordination numbers of the final MoS_2 are higher than that of CoMo/γ-Al_2O_3, suggesting that the MoS_2 edges are more saturated by sulfur and that the crystallites are bigger. This is confirmed by the EXAFS analysis (Table 2). These results suggest that TEG hinders the interaction of heptamolybdate with the alumina support, thus favoring a better polymerization of this species.

The sulfidation of the CoMoP/γ-Al_2O_3 and CoMoP-TEG/γ-Al_2O_3 samples follows a mechanism completely different from that of the phosphate-free catalysts. Phosphate is well known for its beneficial effect on the performance of a supported Co(Ni)Mo catalyst. The effect of phosphate was reviewed and discussed by Iwamoto and Grimblot [24] and Sun et al. [25], who explained that the main role of phosphate is to favor better sulfidation of both the molybdenum and the promoter Co(Ni) atom by weakening the interaction with the alumina support, thus leading to a better catalytic performance. The Mo K-edge QEXAFS of the CoMoP/γ-Al_2O_3 catalyst shows the presence of only two phases: the oxidic phase and the final sulfidic 3R–MoS_2-like phase, as shown from the Mo–S distance of 2.36 Å, typical of the 3R–MoS_2 allotrope [20]. Moreover, the catalyst in the final sulfidic state showed a Mo–S coordination number of 5.8. As expected from the presence of phosphate, the MoS_2 slabs are well sulfided. We cannot exclude the possibility that also in the phosphate-containing catalysts the MoS_3-like phase is an intermediate, and that the phosphate delays its formation to a higher temperature. By the time it starts to form, its decomposition to MoS_2 is already fast, so that the resulting MoS_3 concentration is low and barely detectable.

The CoMoP/γ-Al_2O_3 catalyst showed the lowest Mo–Mo coordination number, indicating a good dispersion. However, judging from the high Mo–Mo Debye–Waller factor (Table 2), the static order was low. This effect can be explained on the basis of previously published results [7,23,24]. Upon impregnation of the support, the phosphomolybdate species that were present in the impregnation solution decompose to aluminum phosphate and aluminum molybdate. Because of the random occurrence of this process, various agglomerations of molybdate species will be present on the alumina surface. Since no calcination was applied, these species remained disordered on the surface of the support, thus causing disorder in the final MoS_2 as well. TEG prevents the phosphomolybdate species from interacting with the support. As a result, these species may precipitate as cobalt salt on the support without undergoing decomposition and redispersion.

The use of TEG together with phosphate had an effect on the sulfidation mechanism of the CoMoP-TEG/γ-Al_2O_3 catalyst precursor. From Fig. 3 it is unclear whether the sulfi-

dation of this catalyst took place in two or three steps. Figs. 4 and 5 give a clearer picture. Fig. 4 shows that, although the sulfidation of CoMoP-TEG/γ-Al_2O_3 started at high temperature (about 200 °C), the eventual Mo–S coordination number is the highest for the four catalysts. This is probably due to the fact that TEG may favor the precipitation of large Co-diphosphopentamolybdate islands over the support, in which both the Mo–O–Mo and the Mo–O–P bonds must be cleaved to obtain the final MoS_2. This can be achieved only when TEG decomposes; this process takes place above 200 °C. At this temperature, the phosphate moiety of the phosphomolybdate can react freely with the alumina surface, for which it has a high affinity, to leave behind the molybdate. This phenomenon is clearly visible in Fig. 3, where the signal between 3.1 and 4.0 Å disappears at 215 °C. Fig. 5 shows that, at this sulfidation temperature, a 3R–MoS_2-like phase formed in the CoMoP-TEG/γ-Al_2O_3 sample. However, at about 300 °C the Mo–S coordination distance increased, indicating a further change in the MoS_2 structure. Finally, at 350 °C the 2H–MoS_2 phase formed (Fig. 5). Table 2 shows that this catalyst has high Mo–S and Mo–Mo coordination numbers and the lowest Mo–Mo Debye–Waller factor, indicating the highest static order.

A check for the presence of various phases in an in situ QEXAFS experiment is the presence of isosbestic points in the spectra. The normalized Mo K-edge XAFS of the CoMo/γ-Al_2O_3 and CoMoP-TEG/γ-Al_2O_3 samples (Fig. 10) shows that only the XAFS of CoMo/γ-Al_2O_3 does not have isosbestic points, indicating that intermediates are involved in the sulfidation of this catalyst. This confirms the QEXAFS analyses.

4.2. Cobalt

The Co K-edge QEXAFS experiments showed that phosphate and TEG have a similar effect on the sulfidation of CoMo-TEG/γ-Al_2O_3, CoMoP/γ-Al_2O_3, and CoMoP-TEG/γ-Al_2O_3. The sulfidation pattern of CoMo/γ-Al_2O_3 was very different, however, as shown by the XANES data as a function of the sulfiding temperature (Fig. 9). The presence of additives strongly modified the local structure of cobalt, such that the sulfidation of Co shifted to lower temperature in the catalyst precursor. A similar trend was found by Cattaneo et al. for the sulfidation of Ni in NiMo/γ-Al_2O_3 catalysts. They explained this by inferring that Ni strongly interacts with the support, and, hence, the sulfidation of Ni is retarded [18]. In the same way, cobalt may react with the support and retard the sulfidation in the CoMo/γ-Al_2O_3 sample.

One of the beneficial effects of phosphate is to hinder the interaction between the catalyst precursors and the alumina support by forming $AlPO_4$. Moreover, we proved that TEG can also react strongly with the alumina support, thus hindering the interaction with the catalyst precursors. These considerations explain the increase in the degree of sulfidation of Co observed for CoMo-TEG/γ-Al_2O_3, CoMoP/γ-Al_2O_3, and CoMoP-TEG/γ-Al_2O_3. Moreover, Cattaneo et al. also observed that the NTA chelating ligand added to NiMo/γ-Al_2O_3 catalysts increased the sulfidation degree of nickel, although this did not result in an increase in the HDS activity [18].

We have to stress that, since calcination of the samples was not applied, the different sulfidation pattern observed in the two sets of catalysts (phosphate-free and containing phosphate) might be partially affected by the NO_3^- and NH_4^+ ions still present in the CoMo/γ-Al_2O_3 and CoMo-TEG/γ-Al_2O_3 oxidic catalysts.

4.3. HDS activity and role of the additives

The activity of HDS catalysts depends strongly on the final sulfidic structure. The CoMo/γ-Al_2O_3 catalyst had the same HDS activity as CoMo-TEG/γ-Al_2O_3. However, the presence of phosphate caused an increase in the HDS activity from the CoMo/γ-Al_2O_3 to the CoMoP/γ-Al_2O_3 sample. The sulfidation profile for the latter catalyst showed that the MoS_2 phase started to form at a lower temperature

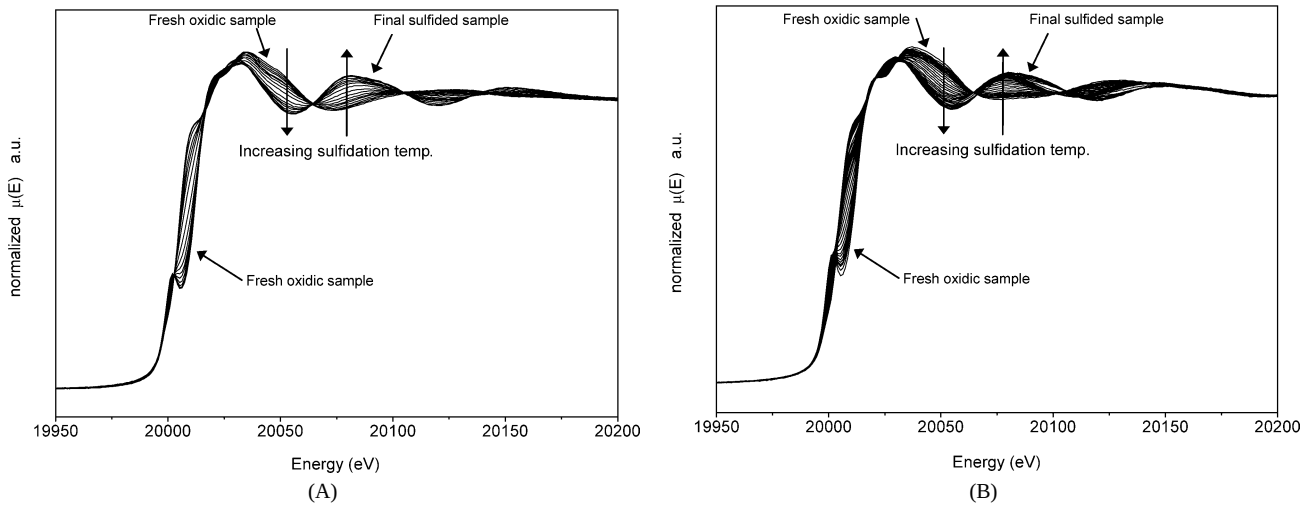

Fig. 10. Normalized in situ Mo K-edge XANES of (A) CoMoP-TEG/γ-Al_2O_3 and (B) CoMo/γ-Al_2O_3 during the heating in a flow of H_2S and H_2.

and that no intermediates were formed. This allowed a better sulfidation of the molybdenum precursor and, therefore, a higher catalytic activity. In the CoMoP-TEG/γ-Al_2O_3 catalyst, the formation of MoS_2 took place at a lower temperature as well. The sulfidation of this sample showed almost the same pattern as that of CoMoP/γ-Al_2O_3, and the catalytic activity was even higher. The presence of both phosphate and TEG prevents the decomposition of the Co-diphosphopentamolybdate species on the alumina support. This facilitates the formation of the most active Co–Mo–S structure, which spreads more homogeneously over the surface of the support. Moreover, the highest MoS_2 static order, as shown by the EXAFS results, supports this explanation.

The sulfidation of cobalt occurs at lower temperature in the presence of either additive. However, the HDS activity is insensitive to this effect, since the activity of the CoMo-TEG/γ-Al_2O_3 catalyst is about the same as that of CoMo/γ-Al_2O_3. This suggests that, in the absence of phosphate, cobalt is not located in the vicinity of molybdenum. Moreover, because of strong interactions with the support, it might not reach the MoS_2 edges and may not attain a good homogeneity of the Co–Mo–S phase. The presence of TEG increases the sulfidation rate of cobalt by limiting the interaction with the support, but it decomposes at about 200 °C. It is not known whether this process has an influence on the local structure of Co, but, as mentioned above, the HDS activity was not affected by the presence of TEG only. Phosphate also prevents a strong interaction between metal precursors and the support and complexes molybdenum and cobalt in a Co-diphosphopentamolybdate species already in the impregnation solution. In the absence of TEG this species decomposes, thus splitting Co and Mo apart on the support. Nevertheless, the advantage of phosphate is that it does not decompose during the sulfidation treatment; therefore, it allows a good sulfidation of the promoter atom along the edges of the MoS_2 slabs. The optimum is reached when, in the presence of TEG, the Co-diphosphopentamolybdate species is preserved, thus keeping Co and Mo in close proximity even on the oxidic catalyst. In this case, the Co–Mo–S phase forms more easily and the catalyst performs best.

5. Conclusions

QEXAFS experiments gave insight into the sulfidation of CoMo/γ-Al_2O_3 and how it is affected by the presence of additives. Our results show that the sulfidation of the classic CoMo/γ-Al_2O_3 catalyst leads to the active MoS_2 phase through the formation of a MoS_3-like phase. In the presence of phosphate this intermediate was not observed and the formation of MoS_2 occurred at lower temperature, favoring a better saturation of the MoS_2 edges. The presence of TEG, in addition to phosphate, improved the static order of MoS_2, thus favoring a better homogeneity of the most catalytically active Co–Mo–S phase. Phosphate and TEG increased the sulfidation rate of cobalt. Nevertheless, this faster sulfidation does not lead to higher HDS activity in the case of TEG. In contrast to the findings of Cattaneo et al. [5,18,23], no correlation was found between late sulfidation of Co and high catalytic activity.

Acknowledgments

The authors thank the staff of the X1 station at HASYLAB for their technical support and their kind help. This project was supported by the Swiss National Science Foundation.

References

[1] B. Scheffer, P. Arnoldy, J.A. Moulijn, J. Catal. 112 (1988) 516.
[2] E. Payen, S. Kasztelan, S. Houssenbay, R. Szymanski, J. Grimblot, J. Phys. Chem. 93 (1989) 6501.
[3] H. Topsøe, B.S. Clausen, F.E. Massoth, Catalysis Science and Technology, Springer, New York, 1996, pp. 1–69.
[4] L. Medici, R. Prins, J. Catal. 163 (1996) 38.
[5] R. Cattaneo, T. Weber, T. Shido, R. Prins, J. Catal. 191 (2000) 225.
[6] M.Y. Sun, T. Bürgi, R. Cattaneo, R. Prins, J. Catal. 197 (2001) 172.
[7] D. Nicosia, R. Prins, J. Catal. 229 (2005) 424.
[8] E. Yamaguchi, Y. Uragami, H. Yokozuka, K. Uekusa, T. Yamaguchi, S. Abe, T. Kamo, T. Suzuki, EP Application 0601722 B1 (1998), Sumitomo Metal.
[9] S.P.A. Louwers, R. Prins, J. Catal. 133 (1992) 94.
[10] R. Frahm, Rev. Sci. Instrum. 60 (1989) 2515.
[11] A. Krolzig, G. Materlik, M. Swars, J. Zegenhagen, Nucl. Instrum. Meth. A 219 (1984) 430.
[12] F.W.H. Kampers, T.M.J. Maas, J. van Grondelle, P. Brinkgreve, D.C. Koningsberger, Rev. Sci. Instrum. 60 (1989) 2635.
[13] M. Vaarkamp, I. Dring, R.J. Oldman, E.A. Stern, D.C. Koningsberger, Phys. Rev. B 50 (1994) 7872.
[14] D.C. Koningsberger, B.L. Mojet, G.E. van Dorssen, D.E. Ramaker, Top. Catal. 10 (2000) 143.
[15] A.L. Ankudinov, B. Ravel, J.J. Rehr, S.D. Conradson, Phys. Rev. B 58 (1998) 7565.
[16] W.L. Dhandapani, S.T. Oyama, Chem. Lett. (1998) 207.
[17] M. Tromp, J.A. van Bokhoven, A.M. Arink, J.H. Bitter, G. van Koten, D.C. Koningsberger, Chem.-Eur. J. 8 (2002) 5667.
[18] R. Cattaneo, F. Rota, R. Prins, J. Catal. 199 (2001) 318.
[19] T. Weber, J.C. Muijsers, H.J.M.C. van Wolput, C.P.J. Verhagen, J.W. Niemantsverdriet, J. Phys. Chem. 100 (1996) 14144.
[20] B. Schönfeld, J.J. Huang, S.C. Moss, Acta Cryst. B 39 (1983) 404.
[21] http://www.fiz-informationsdienste.de/en/DB/icsd/index.html.
[22] T. Shido, R. Prins, J. Phys. Chem. B 102 (1998) 8426.
[23] R. Cattaneo, T. Shido, R. Prins, Stud. Surf. Sci. Catal. 127 (1999) 421.
[24] R. Iwamoto, J. Grimblot, Adv. Catal. 44 (2000) 417.
[25] M. Sun, D. Nicosia, R. Prins, Catal. Today 86 (2003) 173.